J Pharmacol Sci **117**, 243 – 252 (2011)

Journal of Pharmacological Sciences

Full Paper

Platinum Nanoparticles Suppress Osteoclastogenesis Through Scavenging of Reactive Oxygen Species Produced in RAW264.7 Cells

Mayumi Nomura[1,2], Yoshitaka Yoshimura[2,*], Takashi Kikuiri[3], Tomokazu Hasegawa[4], Yumi Taniguchi[3], Yoshiaki Deyama[2], Ken-ichi Koshiro[5], Hidehiko Sano[5], Kuniaki Suzuki[2], and Nobuo Inoue[1]

[1]*Department of Gerodontology,* [2]*Department of Molecular Cell Pharmacology,* [3]*Department of Pediatric Dentistry, and* [5]*Department of Restorative Dentistry, Hokkaido University Graduate School of Dental Medicine, Kita-ku, Sapporo 060-8586, Japan*

[4]*Department of Pediatric Dentistry, Faculty of Dentistry, Tokushima University, 3-18-15, Kuramoto-cho, Tokushima 770-8504, Japan*

Received June 6, 2011; Accepted October 6, 2011

Abstract. Recent research has shown that platinum nanoparticles (nano-Pt) efficiently quench reactive oxygen species (ROS) as a reducing catalyst. ROS have been suggested to regulate receptor activator of NF-κB ligand (RANKL)-stimulated osteoclast differentiation. In the present study, we examined the direct effects of platinum nano-Pt on RANKL-induced osteoclast differentiation of murine pre-osteoclastic RAW 264.7 cells. The effect of the nano-Pt on the number of osteoclasts was measured and their effect on the mRNA expression for osteoclast differentiation was assayed using real-time PCR. Nano-Pt appeared to have a ROS-scavenging activity. Nano-Pt decreased the number of osteoclasts (2+ nuclei) and large osteoclasts (8+ nuclei) in a dose-dependent manner without affecting cell viability. In addition, this agent significantly blocked RANKL-induced mRNA expression of osteoclastic differentiation genes such as c-fms, NFATc1, NFATc2, and DC-STAMP as well as that of osteoclast-specific marker genes including MMP-9, Cath-K, CLC7, ATP6i, CTR, and TRAP. Although nano-Pt attenuated expression of the ROS-producing NOX-family oxidases, Nox1 and Nox4, they up-regulated expression of Nox2, the major Nox enzyme in macrophages. These findings suggest that the nano-Pt inhibit RANKL-stimulated osteoclast differentiation via their ROS scavenging property. The use of nano-Pt as scavengers of ROS that is generated by RANKL may be a novel and innovative therapy for bone diseases.

Keywords: platinum nanoparticle, osteoclast, reactive oxygen species (ROS), NOX, RAW cell

Introduction

Bone is continuously remodeled by osteoblasts and osteoclasts (1 – 3). The proper balance between bone formation and resorption is regulated by various hormones and cytokines that modulate bone metabolism. If this balance is disrupted, metabolic bone diseases such as osteoporosis and osteopetrosis result (4, 5). Osteoclasts are members of the monocyte/macrophage lineage and are formed by fusion of their mononuclear cellular precursors. The receptor activator of NF-κB (RANK) ligand (RANKL) is the most essential cytokine for the process of osteoclast differentiation and activation (6). RANKL is a member of the tumor necrosis factor (TNF) family and is expressed as a membrane-bound protein in osteoblasts and stromal cells (1). The receptor for RANKL, termed RANK, is induced by macrophage colony–stimulating factor (M-CSF) in osteoclast precursor cells. M-CSF is also an essential factor for the survival of osteoclast precursor cells and for the formation of osteoclasts (7). The pre-osteoclastic RAW264.7 cells we used in this study express endogenous RANK and can differentiate into osteoclasts following RANKL stimulation without M-CSF. Binding of RANKL to RANK induces activa-

*Corresponding author. yoshi@den.hokudai.ac.jp
Published online in J-STAGE on November 12, 2011 (in advance)
doi: 10.1254/jphs.11099FP

tion of TNF receptor–associated factor 6 (TRAF6) and c-Fos pathways, which lead to auto-amplification of nuclear factor of activated T cells (NFAT) c1, the master transcription factor for osteoclast differentiation. Auto-amplification of NFATc1 is also dependent on calcium signaling and regulates many osteoclast marker genes such as cathepsin K, tartrate-resistant acid phosphatase (TRAP) and the calcitonin receptor (8).

A variety of cytokines and growth factors have been shown to generate reactive oxygen species (ROS) (9). Although high concentrations of ROS cause oxidative stress injury that is implicated in the pathogenesis of different types of diseases, ROS also play a role as second messengers in signaling pathways that participate in a variety of cellular functions (10). ROS generated by osteoclasts are suggested to take part in the complex process of bone resorption (11, 12). Following stimulation with RANKL, osteoclast precursors increase intracellular ROS by activation of NADPH oxidase (Nox) homologs (13) or by increasing mitochondrial ROS production (14). In addition, a recent study indicated that *N*-acetylcysteine, a chemical oxidant scavenger, blocks RANKL-induced ROS production and osteoclastogenesis (13). These reports suggested that ROS are essential for the formation and function of osteoclasts and regulate RANKL-stimulated osteoclast differentiation (13, 15).

Platinum nanoparticles (nano-Pt) have attracted attention in recent years due to the fact that they have been shown to scavenge ROS persistently and catalytically (16). Nano-Pt are colloids of nano-sized particles of platinum, which are added to health foods or cosmetics due to their antioxidation and anti-aging properties (17). Although other antioxidants can only scavenge specific types of reactive oxygen, nano-Pt can function as reductive catalysts to scavenge all types of ROS. It has been suggested that nano-Pt scavenge ROS by functioning as a superoxide dismutase (SOD) / catalase mimetic (18, 19). However, although there have been several studies regarding the biological effects of nano-Pt, it is unknown whether nano-Pt have a direct effect on osteoclast differentiation. Therefore, in the present study, we investigated the effect of nano-Pt on osteoclast differentiation.

Materials and Methods

Measurement of ROS

To detect ROS formed in the Fenton reaction, we used 2-[6-(4′-amino) phenoxy-3*H*-xanthen-3-on-9-yl]benzoic acid (APF; Sekisui Medical, Tokyo). APF is a novel fluorescence probe that specifically detects highly reactive oxygen species (hROS) such as hydroxyl radicals (•OH) as well as reactive intermediates of peroxidase in the form of an increase in fluorescence (20). To generate ROS, H_2O_2 (0, 2.5, or 5 μM) was incubated in sodium phosphate buffer containing 2 μM horseradish peroxidase (HRP; Wako Pure Chemicals, Osaka) for 20 min at 37°C in the dark. The nano-Pt (0, 10, or 100 μM) were then added and incubated for 10 min under the same conditions. Finally, APF (100 μM) was added and the fluorescence intensity was determined at 535 nm, with excitation at 485 nm, using a microplate reader (Wallac 1420 ARVOsx; Perkin Elmer, Waltham, MA, USA).

Preparation of the nano-Pt

The nano-Pt were a gift from Apt Co., Ltd. (Tokyo) and prepared by the citrate reduction of H_2PtCl_6 (21). The average diameter of the nano-Pt was 2.0 nm, and the nano-Pt were dissolved in a large quantity of a citric acid solution. To compare the effect of ROS scavenging, we used other ROS scavengers, *N*-acetylcysteine (NAC; Sigma-Aldrich, St. Louis, MO, USA) and GSH (Wako).

Cell culture

The murine monocyte/macrophage cell line RAW264.7 (RAW) (ATCC, Manassas, VA, USA) was used as osteoclast precursor cells. RAW cells differentiate into osteoclast-like cells in the presence of RANKL. The cells were grown in Dulbecco's Modified Eagle's medium (DMEM, Wako), supplemented with 10% (v/v) heat-inactivated fetal bovine serum (FBS) (Invitrogen, Carlsbad, CA, USA) and 66.7 μg/ml kanamycin-sulfate (Meiji Seika, Tokyo) at 37°C in a humidified atmosphere of 95% air and 5% CO_2. The cells were seeded onto 100-mm standard dishes (BD Falcon, Franklin Lakes, NJ, USA). After overnight culture, RAW cells were transferred into 48-well culture plates (BD) at a density of 0.5×10^4 cells/well with α-minimum essential medium (α-MEM) supplement with 10% heat-inactivated FBS, 50 ng/ml RANKL (Oriental Yeast, Tokyo), 284 μM L-ascorbic acid 2-phosphate (Sigma-Aldrich), 2 mM L-alanyl-L-glutamine (Sigma-Aldrich), and 66.7 μg/ml kanamycin-sulfate at 37°C in a humidified atmosphere of 95% air and 5% CO_2 and were then treated with different reagents. The medium containing these reagents was replaced every other day.

Bone marrow cells were prepared as previously described by Hu et al. (22). For the experiments of osteoclastogenesis in bone marrow macrophages (BMMs), freshly prepared bone marrow cells were incubated in 100-mm standard dishes with α-MEM containing 10% FBS, as described above, in the presence of 10 ng/ml M-CSF (PeproTech, Rocky Hill, NJ, USA) for 1 day. The nonadherent cells were collected and counted. BMMs were replated in 48-well culture plates at a density of 2×10^4 cells/well and incubated in the presence of M-CSF (30 ng/ml) and RANKL (50 ng/ml) and were

then treated with different reagents for 7 days. The medium containing these reagents was replaced every other day.

Animal care and experimental procedures were performed in accordance with the Guidelines for Animal Experimentation of Hokkaido University with approval of the Institutional Animal Care and Use Committee.

TRAP staining

Cells cultured for a given period were washed with PBS and fixed in 10% neutral formalin. They were then washed with distilled water and stained with Fast Red Violet LB Salt (Sigma-Aldrich). After washing, TRAP-positive cells with more than two nuclei were considered to be osteoclast-like cells and osteoclasts with 8 nuclei or more were considered to be large osteoclasts (23). The number of osteoclasts was counted under a light microscope.

Analysis of cytotoxicity

The cytotoxicity of Pt was analyzed by using the Cell Counting Kit-8 (Dojindo Molecular Technologies, Inc., Kumamoto). Hydrogen hexachloroplatinate (H_2PtCl_6) (Apt) was diluted with distilled water. RAW cells were seeded on a 96-well plate at a density of 0.2×10^4 cells/well with different reagents. After 6 days of culture, the medium was changed to new medium (100 μl) and 10 μl of the Cell Counting Kit-8 solution was added. After incubation for 2 h at 37°C, the absorbance was measured at 450 nm using a microplate reader (Model 550; Biorad, Hercules, CA, USA) and the background reading (medium) was subtracted.

Quantitative real-time PCR

RAW cells were seeded on a 6-well plate at a density of 5×10^4 cells/well and were treated with different reagents for 5 days. Total RNA was extracted using Trizol (Invitrogen) according to the manufacturer's instructions. cDNA was synthesized from 1 μg of total RNA using ReverTra Ace reverse transcriptase (TOYOBO, Osaka) and oligo dT primers (TOYOBO).

We used specific primers for analysis of the mRNA of the osteoclastogenic proteins: RANK, M-CSF receptor (c-fms), NFATc1, NFATc2, NFATc3, and dendritic cell-specific transmembrane protein (DC-STAMP); the osteoclast specific markers: matrix metalloproteinase-9 (MMP-9), cathepsin-K (Cath-K), chloride channel 7(CLC-7), ATPase (ATP6i), calcitonin receptor (CTR), and TRAP; and of Nox enzymes and their partner proteins: Nox1, Nox2, Nox3, Nox4, Nox organizer 1 (NOXO1), Nox activator 1 (NOXA1), $p47^{phox}$, $p67^{phox}$, $p22^{phox}$, Rac1, and Rac2. The specific primer sets used for RANK (Mm00437135_m1), c-fms (Mm00432689_m1), NFATc1 (Mm00479445_m1), NFATc2 (Mm004777776_m1), NFATc3 (Mm01249194_m1), DC-STAMP (Mm01168058_m1), MMP-9 (Mm00442991_m1), Cath-K (Mm00484036_m1), CLC-7 (Mm00442400_m1), ATP6i (Mm00469395_m1), CTR (Mm00432271_m1), TRAP (Mm00475698_m1), Nox1 (Mm01340621_g1), Nox2 (Mm00432774_m1), Nox3 (Mm01339126_m1), Nox4 (Mm00479246_m1), NOXO1 (Mm00546832_g1), NOXA1 (Mm00549171_m1), $p47^{phox}$ (Mm00447921_m1), $p67^{phox}$ (Mm00726636_s1), $p22^{phox}$ (Mm00514478_m1), Rac1 (Mm01201653_mH), Rac2 (Mm00485472_m1), and glyceraldehyde 3-phosphate dehydrogenase (GAPDH) (Mm99999915_g1) were designed using the Primer Express program (Applied Biosystems, Foster City, CA, USA) and were purchased from Applied Biosystems. Quantitative real-time PCR was performed using the ABI 7300 (Applied Biosystems).

We used the comparative Ct method to calculate mRNA expression. We verified the Ct values of both the calibrator and the samples of interest by normalizing them to GAPDH. The comparative Ct method is also known as the $2^{-\Delta\Delta Ct}$ method, where, $\Delta Ct = \Delta Ct$, sample $- \Delta Ct$, reference. ΔCT, sample is the Ct value for the samples normalized to the endogenous housekeeping gene, and ΔCt, reference is the Ct value for the calibrator, which was also normalized to the endogenous housekeeping gene.

Statistical analysis

All data are expressed as mean ± S.D. Comparisons between samples of interest and the respective controls were analyzed using the 2-tailed unpaired Student's *t*-test. *P* values of < 0.05 were considered to be statistically significant.

Results

Antioxidant property of nano-Pt

We used APF as a novel fluorescence probe for detection of ROS production. We first used APF to analyze the antioxidant properties of nano-Pt in solution. For this purpose, we generated hROS from H_2O_2 in phosphate buffer (pH 7.4) containing HRP. As shown in Fig. 1, the fluorescence intensity of APF increased in proportion to the concentration of H_2O_2 due to APF-ROS reactivity. The nano-Pt dose-dependently inhibited this increase in fluorescence intensity and 100 μM nano-Pt completely inhibited this increase in fluorescence intensity. This result shows that nano-Pt scavenge ROS in a dose-dependent manner.

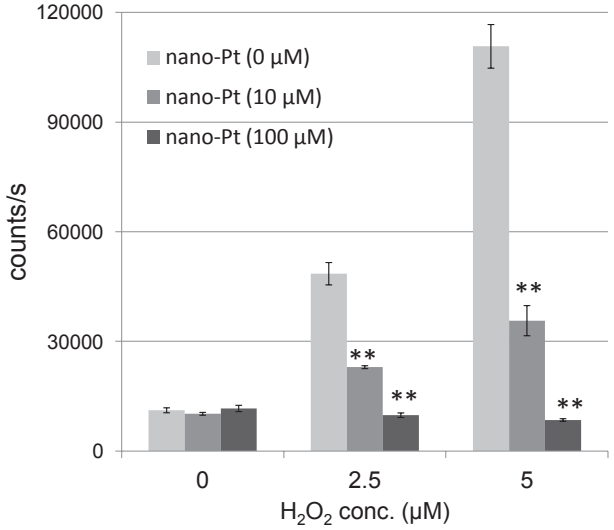

Fig. 1. Antioxidant property of nano-Pt. H_2O_2 (0, 2.5, or 5 μM) was incubated in sodium phosphate buffer containing HRP (2 μM) for 20 min at 37°C in the dark. Nano-Pt (0, 10, or 100 μM) were then added and incubated for 10 min under the same conditions. Finally, APF (100 μM) was added and fluorescence intensity was determined at 535 nm, with excitation at 485 nm, using a microplate reader. Results are shown as the mean ± S.D. for 4 independent experiments. $^{**}P < 0.01$, significant difference from same H_2O_2 concentrations of the control (nano-Pt 0 μM).

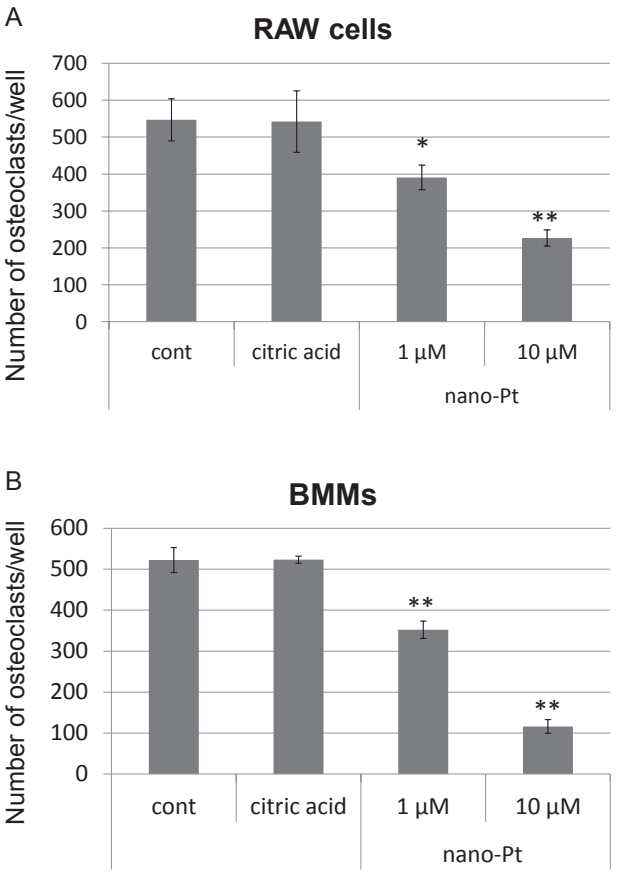

Fig. 2. Effect of citric acid contained within nano-Pt on osteoclast differentiation. RAW cells (0.5×10^4 cells/well) were cultured on 48-well plates without citric acid (cont) or with citric acid, 1 or 10 μM nano-Pt in the presence of RANKL. After 6 days of culture, the number of osteoclasts was counted. Results are shown as the mean ± S.D. for 3 independent experiments (A). BMMs (2×10^4 cells/well) were cultured on 48-well plates without citric acid (cont) or with citric acid, 1 or 10 μM nano-Pt in the presence of M-CSF and RANKL. After 7 days of culture, the number of osteoclasts was counted. Results are shown as the mean ± S.D. for 3 independent experiments (B). $^{*}P < 0.05$, $^{**}P < 0.01$, significant difference from untreated control cells.

Effect of citric acid contained within nano-Pt on osteoclast differentiation

Because the nano-Pt were dissolved in a citric acid solution, we examined the influence of citric acid alone as well as the effect of nano-Pt dissolved in it on osteoclastic differentiation of RAW cells and BMMs. Differentiation was induced by RANKL addition and was measured by counting the number of osteoclasts. There were no differences in the number of osteoclasts between control cells and cells cultured in citric acid for both RAW cells and BMMs (Fig. 2: A, B). In contrast, nano-Pt strongly inhibited osteoclast differentiation in a concentration-dependent manner. In addition, an ATP bioluminescence assay indicated that neither citric acid nor the nano-Pt affected RAW cell growth (data not shown). These results suggested that the effect of the nano-Pt on osteoclast differentiation was due to the nano-particle itself and not to citric acid.

Effect of the nano-Pt on the number of TRAP-positive multinucleated osteoclasts

We further analyzed the effect of nano-Pt on osteoclast differentiation by incubating RAW cells with different concentrations of the nano-Pt (0, 1, or 10 μM) together with RANKL and counting both the number of osteoclasts and the number of large osteoclasts that appeared over a period of 9 days. Both osteoclasts and large osteoclasts appeared on day 4, and their number continued to increase up to day 6. Although there were no different osteoclast morphologies between the presence of nano-Pt and the absence of them, the nano-Pt strongly and dose-dependently decreased the number of osteoclasts on all culture days (Fig. 3A). Compared with the control, 10 μM nano-Pt suppressed osteoclastogenesis by 45% on day 5 and by 40% on day 6. Likewise, the number of large osteoclasts with > 8 nuclei was significantly decreased by the nano-Pt (Fig. 3B). Large osteoclasts accounted for 30% of the total osteoclasts in the control and for 12% in the cells to which 10 μM nano-Pt had been

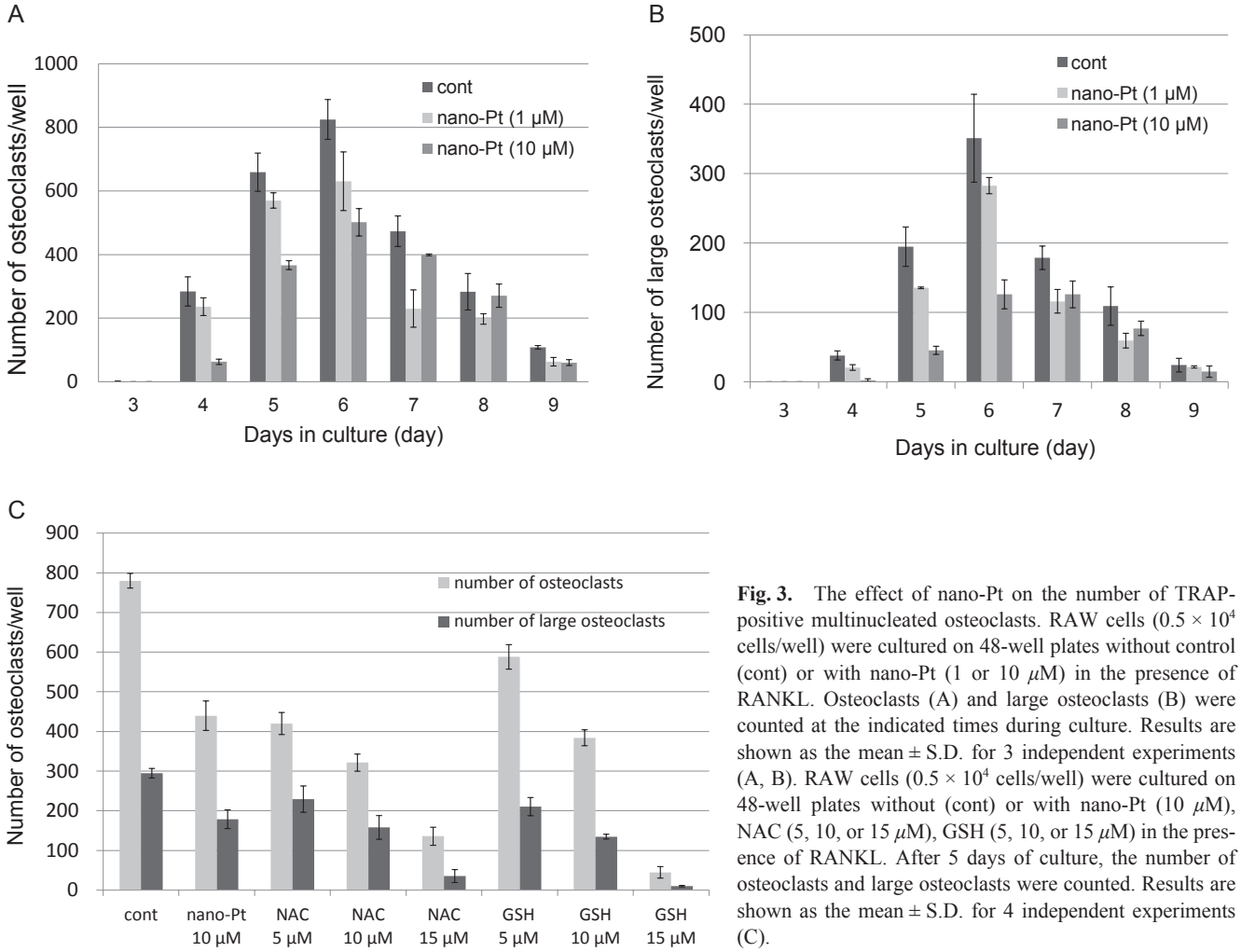

Fig. 3. The effect of nano-Pt on the number of TRAP-positive multinucleated osteoclasts. RAW cells (0.5×10^4 cells/well) were cultured on 48-well plates without control (cont) or with nano-Pt (1 or 10 μM) in the presence of RANKL. Osteoclasts (A) and large osteoclasts (B) were counted at the indicated times during culture. Results are shown as the mean ± S.D. for 3 independent experiments (A, B). RAW cells (0.5×10^4 cells/well) were cultured on 48-well plates without (cont) or with nano-Pt (10 μM), NAC (5, 10, or 15 μM), GSH (5, 10, or 15 μM) in the presence of RANKL. After 5 days of culture, the number of osteoclasts and large osteoclasts were counted. Results are shown as the mean ± S.D. for 4 independent experiments (C).

added on day 5. The respective percentages were 43% in the control and 25% in the 10 μM nano-Pt–treated group on day 6. These findings indicate that addition of the nano-Pt not only suppressed osteoclast differentiation, but also suppressed the fusion of osteoclasts. In addition, another ROS scavenger, NAC and GSH, also decreased the number of osteoclasts and large osteoclasts. These results suggest that scavenging effects of ROS inhibit osteoclast differentiation (Fig. 3C).

Effect of Pt-induced cytotoxicity on osteoclast differentiation

Because Pt is known to be cytotoxic, we determined whether Pt cytotoxicity played a role in the nano-Pt–induced suppression of osteoclast differentiation. Since Pt is water and alcohol-insoluble we used H_2PtCl_6, which can be dissolved in deionized water, in order to analyze Pt cytotoxicity. RAW cells did not survive in the presence of H_2PtCl_6 (Fig. 4), indicating that H_2PtCl_6 was cytotoxic and induced cell death. In contrast, none of the other reagents tested, including the nano-Pt themselves, caused any significant change in the survival of RAW cells.

Effect of the nano-Pt on the mRNA expression of osteoclastic differentiation genes in RAW cells

To investigate the effect of the nano-Pt on the mRNA expression of genes associated with osteoclastogenesis, we cultured RAW cells for 5 days in the presence of RANKL and analyzed the mRNA expression of these genes using real time PCR analysis. The osteoclastogenic genes whose mRNA expression we examined were the following: RANK, c-fms, NFATc1, NFATc2, NFATc3, and DC-STAMP. The 10 μM nano-Pt reduced the mRNA expression of NFATc1, an essential factor for osteoclastic differentiation, as well as of NFATc2 (Fig. 5). In addition, the mRNA expression of c-fms and DC-STAMP was also decreased. However, the nano-Pt did not affect the mRNA expression of RANK and NFATc3.

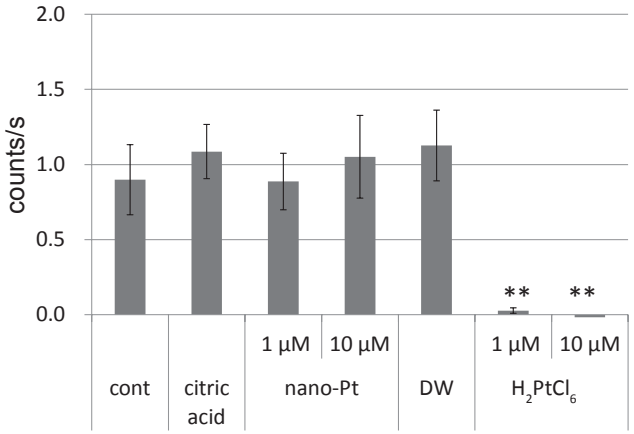

Fig. 4. Effect of nano-Pt–induced cytotoxicity on osteoclast differentiation. RAW cells (0.2×10^4 cells/well) were cultured on 96-well plates with or without citric acid, nano-Pt (1 or 10 μM), distilled water (DW), or H_2PtCl_6 (1 or 10 μM) in the presence of RANKL. After 6 days of culture, the medium (100 μl) was changed to fresh medium and 10 μl of the Cell Counting Kit-8 solution was added. After incubation for 2 h at 37°C, absorbance was measured at 450 nm using a microplate reader. Results are adjusted for background (medium) and shown as the mean ± S.D. for 3 independent experiments. $^{**}P < 0.01$, significant difference from untreated control cells.

Effect of the nano-Pt on the mRNA expression of osteoclast-specific markers in RAW cells

We further examined the effect of the nano-Pt on the mRNA expression of osteoclast-specific marker genes (MMP-9, Cath-K, CLC7, ATP6i, CTR, and TRAP), which are markers that differentiate mature from non-differentiated osteoclasts. The 10 μM nano-Pt markedly inhibited the expressions of marker genes and the expression levels of Cath-K and CLC7 were also attenuated by 1 μM nano-Pt. Although the number of osteoclast and large osteoclast were decreased by 1 μM nano-Pt, there were no significant differences in the mRNA expression of MMP-9, ATP6i, CTR, and TRAP from the control (Fig. 6).

Effect of the nano-Pt on the mRNA expression of Nox enzymes and their partner proteins in RAW cells

Nox proteins are membrane-associated multi-unit enzymes that generate ROS by transferring an electron from NADPH to molecular oxygen. The Nox family is composed of Nox1, Nox2 ($gp91^{phox}$), Nox3, Nox4, and Nox5, all of which require a regulatory protein such as NoxO1, NoxA1, $p47^{phox}$, $p67^{phox}$, $p22^{phox}$, Rac1, and Rac2 in order to form the active enzyme and they have distinct functions (24 – 26). We investigated the effect of nano-Pt on the mRNA expression of nox enzymes and their

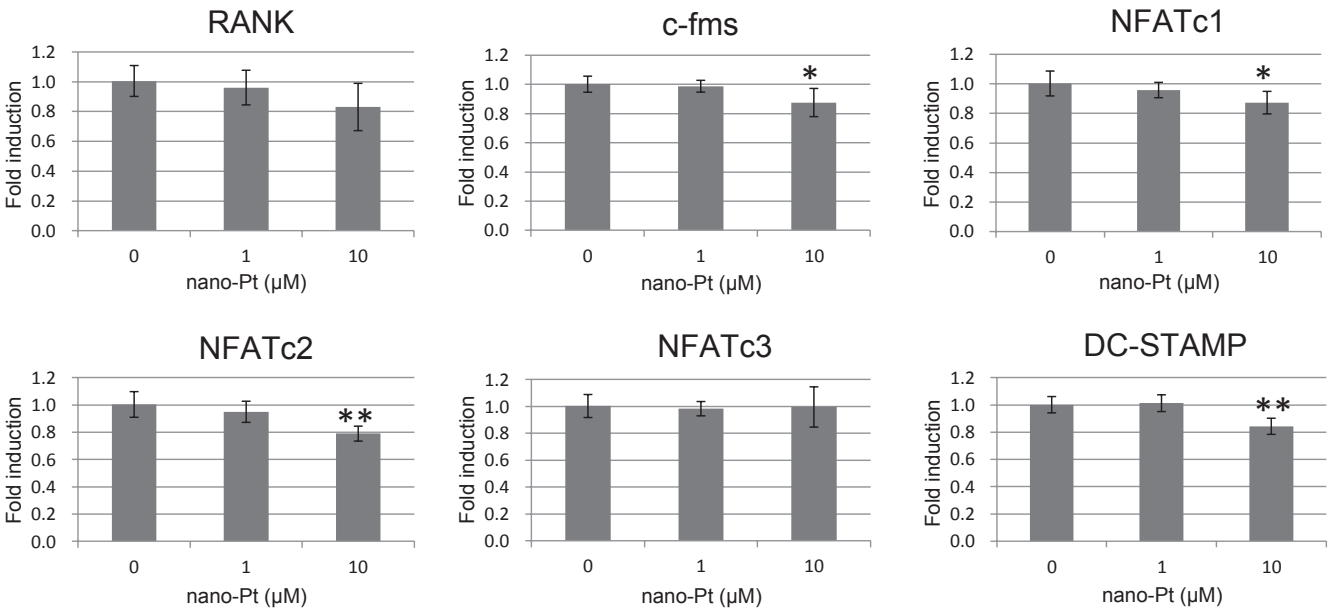

Fig. 5. Effect of nano-Pt on the mRNA expression of osteoclast differentiation genes in RAW cells. RAW cells (5×10^4 cells/well) were cultured on a 6-well plate with RANKL, with or without nano-Pt (0, 1, or 10 μM) for 5 days. Transcript levels of RANK, c-fms, NFATc1, NFATc2, NFATc3, and DC-STAMP were measured using real-time PCR analysis and specific primers. The results are displayed as fold induction, which was calculated relative to the control using the comparative Ct method after normalization against GAPDH expression and as the mean ± S.D. of four independent experiments. $^{*}P < 0.05$, $^{**}P < 0.01$, significant difference from untreated control cells.

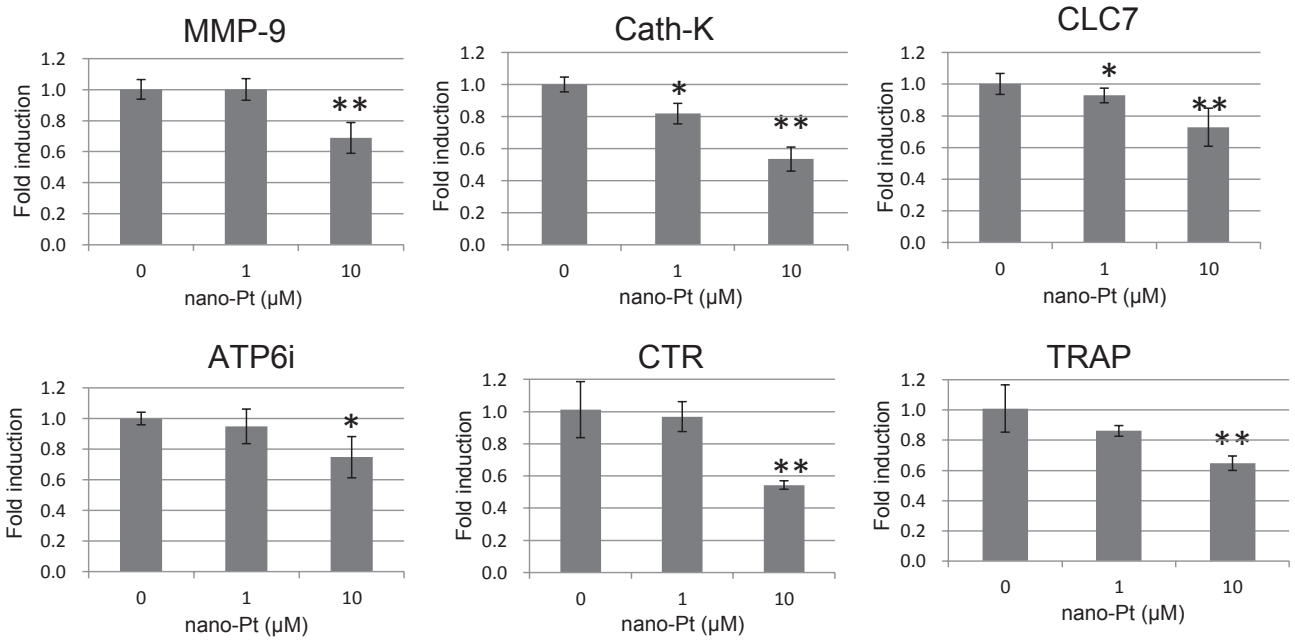

Fig. 6. Effect of nano-Pt on the mRNA expression of osteoclast-specific markers in RAW cells. RAW cells (5×10^4 cells/well) were cultured on a 6-well plate with RANKL, with or without nano-Pt (0, 1, or 10 μM) for 5 days. Transcript levels of MMP-9, Cath-K, CLC-7, ATP6i, CTR, and TRAP were measured using real-time PCR analysis and specific primers. The results are displayed as fold induction relative to the control, which was calculated using the comparative Ct method after normalization against GAPDH expression and as the mean ± S.D. of four independent experiments. *$P < 0.05$, **$P < 0.01$, significant difference from untreated control cells.

partner proteins in RAW cells in the presence of RANKL. Treatment with nano-Pt decreased the mRNA level of Nox1, Nox4, and NOXO1 mRNA (Fig. 7). The mRNA expression of Nox1 and Nox4 mRNA was inhibited by 50% by 10 μM nano-Pt. In contrast, nano-Pt significantly up-regulated the Nox2 mRNA level. The mRNA expression of $p47^{phox}$, $p67^{phox}$, $p22^{phox}$, Rac1, and Rac2 was not affected by treatment with nano-Pt. We also confirmed that NOX3 and NOXA1 transcripts were not detectable (data not shown).

Discussion

It is well known that the accumulation of molecular damage caused by free radicals derived from ROS is one of the key factors in aging (27 – 29). Antioxidant therapy is therefore considered an effective medical treatment for aging. It has been shown that nano-Pt can function as a strong, stable reducing catalyst that efficiently quenches ROS (16). Since the use of platinum as a food additive has been approved, commercial products supplemented with nano-Pt have been marketed in Japan as antioxidants (17). In contrast to ROS-induced damage, recent studies indicate that small amounts of ROS may function as a second messenger in various receptor signaling pathways (10). Thus, for example, ROS have been suggested to regulate RANKL-stimulated osteoclast differentiation and function. In the present study, we investigated the effect of nano-Pt on osteoclast differentiation. We first verified that nano-Pt have antioxidant capacity using the fluorescent probe APF. Indeed, the fluorescence intensity of APF that was increased due to reactivity of APF with ROS was inhibited by nano-Pt (Fig. 1) and nano-Pt quenched ROS production in a dose-dependent manner.

To examine the direct effect of nano-Pt on RANKL-stimulated osteoclast differentiation, RAW cells and BMMs were cultured with nano-Pt. For both RAW cells and BMMs, nano-Pt prominently reduced the number of osteoclasts (Fig 2: A, B). However, because the aim of this study was to investigate the effect of nano-Pt on RANKL-induced osteoclastogenesis, we used RAW cells that express endogenous RANK and can differentiate into osteoclasts following only RANKL-stimulation following experiments. Addition of nano-Pt to RAW cells undergoing osteoclast differentiation induced by RANKL led to a significant decrease in the number of osteoclasts in a nano-Pt concentration–dependent manner (Fig. 3A). Likewise, the number of large osteoclasts was also suppressed by addition of nano-Pt (Fig. 3B). However, we observed no difference in the peak number of

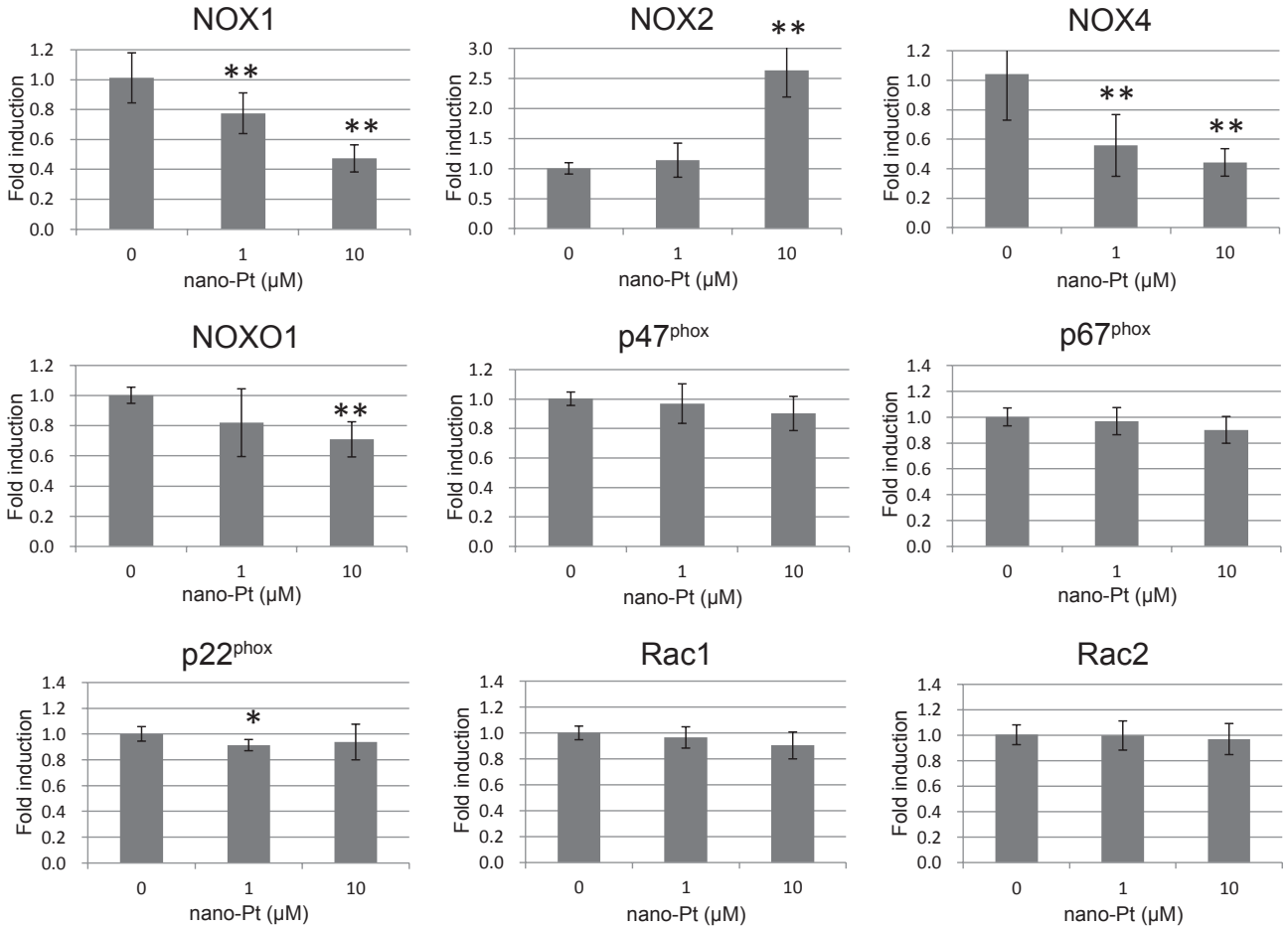

Fig. 7. Effect of nano-Pt on the mRNA expression of NOX enzymes and their partner proteins in RAW cells. AW cells (5×10^4 cells/well) were cultured on a 6-well plate with RANKL, with or without nano-Pt (0, 1, or 10 μM) for 5 days. Transcript levels of NOX1, NOX2, NOX4, NOXO1, $p47^{phox}$, $p67^{phox}$, $p22^{phox}$, Rac1, and Rac2 were measured using real-time PCR analysis and specific primers. The results are displayed as fold induction, which was calculated using the comparative Ct method relative to the control after normalization against GAPDH expression and as the mean ± S.D. of four independent experiments. *$P < 0.05$, **$P < 0.01$, significant difference from untreated control cells.

large osteoclasts with any concentration of nano-Pt tested (Fig 3: A, B). This result indicates that nano-Pt do not delay, but inhibit, osteoclast differentiation and fusion (13, 15).

The cytotoxicity of platinum has been well established. Cisplatin, which is an effective antineoplastic agent, is cytotoxic and causes serious adverse effects. Therefore, it was suspected that the cytotoxicity of platinum might contribute to the suppression of osteoclast differentiation. Nevertheless, although the cytotoxicity of H_2PtCl_6 induced cell death, nano-Pt were not cytotoxic, even at a concentration of 10 μM. These results suggested that the effect of nano-Pt on osteoclast differentiation was not due to the cytotoxicity of platinum.

We further investigated the effect of the nano-Pt on the mRNA expression of osteoclast associated genes in RAW cells. The expression of NFATc1 mRNA was decreased by addition of nano-Pt (Fig. 5). NFATc1 is a master regulator of RANKL-induced osteoclast differentiation and plays a pivotal role in osteoclast fusion and osteoclast activation via up-regulation of various osteoclast-related genes (8, 30). Therefore, suppression of NFATc1 mRNA by nano-Pt indicates inhibition of osteoclast differentiation (8). The mRNA level of NFATc2 that activates the initial induction of NFATc1 was also decreased by nano-Pt. NFATc1 has been shown to regulate the expression of osteoclast marker genes (6). Nano-Pt at 10 μM also inhibited the mRNA expression of osteoclast specific markers and this suppression corresponded to the nano-Pt–induced decrease in the number of osteoclasts. Furthermore, recent reports demonstrate that NFATc1 induces osteoclast fusion via up-regulation

of the DC-STAMP (31), which is essential for cell-cell fusion in osteoclasts (32). In this study, nano-Pt reduced the expression of DC-STAMP mRNA in addition to that of NFATc1. These results suggest that nano-Pt inhibit osteoclast differentiation and fusion via down-regulation of NFATc1 signaling. However, compared with the decrease in the number of osteoclasts, the addition of 1 μM nano-Pt induced little significant difference in the mRNA expression of osteoclast-associated genes and marker genes from the control. Although the mRNA expressions of osteoclast marker genes do not always correlate with the number of osteoclasts (33, 34), this discrepancy indicates that other factors may be involved in the effect of nano-Pt on osteoclast differentiation. To identify such factors, we examined the expression of Nox enzymes and their partner proteins during RANKL-induced osteoclast differentiation and the effect of nano-Pt on these enzymes. Nox is an enzyme system that has been shown to generate ROS in osteoclasts (35, 36). Nox2 is the main Nox enzyme expressed in osteoclast precursors. Nox1 is expressed at a low level and other Nox family members such as Nox3 and Nox4 are not expressed. A recent study demonstrated that the level of ROS rapidly increased to its maximum level after RANKL addition and thereafter decreased towards its basal level (13). This decline in ROS-producing capability was associated with a reduction in Nox2 mRNA expression (37). As RANKL decreased Nox2 mRNA levels, it inversely increased Nox1 mRNA levels (13) and newly induced Nox4 transcript expression (38, 39). It has been shown that Nox1 plays a role in RANKL-induced osteoclast differentiation and Nox4 is involved in bone resorption by osteoclasts (13, 36, 37). These findings suggest that terminal differentiation of osteoclasts is associated with a switch from the potent Nox2-based oxidase system to functionally different Nox systems and that this switch is sufficient to change intracellular signals and cellular functions (35). Real-time PCR analysis showed that Nox2 mRNA expression was significantly increased depending on the concentration of nano-Pt used. In contrast, nano-Pt dose-dependently inhibited Nox1 and Nox4 mRNA expression. These results suggest that Nox2 is up-regulated during the process of osteoclast differentiation due to the antioxidant property of nano-Pt. The lack of attenuation of the potent Nox2-based oxidase system may lead to inhibition of Nox1 and Nox4 expression and osteoclast formation. This down regulation of Nox1 and Nox4 may participate in the suppression of osteoclast differentiation. However, although the NADPH oxidase system is a major contributing factor in RANKL-stimulated ROS production and osteoclast differentiation, it has also been shown that mitochondrial function and intramitochondrial ROS play important roles in osteoclastogenesis (14). Therefore further studies are necessary to address the signaling mechanisms of nano-Pt in more detail.

In summary, this is the first study of the direct effects of nano-Pt on RANKL-induced osteoclast differentiation. We found that nano-Pt inhibited RANKL-stimulated osteoclast differentiation in RAW cells due to its antioxidant property. Although further studies are needed, our data indicate that the application of nano-Pt as scavengers or inhibitors of RANKL-induced ROS generating pathways may be beneficial strategies for alternative therapy of age-related and bone diseases such as osteoporosis.

Acknowledgments

We are grateful to Drs. M. Uo and K. Shibata for technical advice and support. This study was supported in part by Japan Society for the Promotion of Science; Grant-in-Aid for Scientific Research (C) 22592274 to YY and 21592584 to TK and Grant-in-Aid for Young Scientists (B) 22792032 to YT.

References

1 Boyle WJ, Simonet WS, Lacey DL. Osteoclast differentiation and activation. Nature. 2003;423:337–342.
2 Suda T, Takashi N, Udagawa N, Jimi E, Gillespie MT, Martin TJ. Modulation of osteoclast differentiation and function by the new members of the tumor necrosis factor receptor and ligand families. Endocr Rev. 1999;20:345–357.
3 Teitelbaum SL. Bone resorption by osteoclasts. Science. 2000; 289:1504–1508.
4 Yang S, Ries WL, Key LL. Superoxide generation in transformed B-lymphocytes from patients with severe, malignant osteopetrosis. Mol Cell Biochem. 1999;199:15–24.
5 Suzuki A, Sekiguchi S, Asano S, Itoh M. Pharmacological topics of bone metabolism: recent advances in pharmacological management of osteoporosis. J Pharmacol Sci. 2008;106:530–535.
6 Vaananen HK, Laitala-Leinonen T. Osteoclast lineage and function. Arch Biochem Biophys. 2008;473:132–138.
7 Yoshida H, Hayashi S, Kunisada T, Minetaro O, Nishikawa S, Okamura H, et al. The murine mutation osteopetrosis is in the coding region of the macrophage colony stimulating factor gene. Nature. 1990;345:442–444.
8 Takayanagi H. The role of NFAT in osteoclast formation. Ann N Y Acad Sci. 2007;1116:227–237.
9 Thannickal VJ, Fanburg BL. Reactive oxygen species in cell signaling. Am J Physiol Lung Cell Mol Physiol. 2000;279: L1005–L1028.
10 Harris ML, Schiller HJ, Reilly PM, Donowitz M, Grisham MB, Bulkley GB. Free radicals and other reactive oxygen metabolites in inflammatory bowel disease: cause, consequence or epiphenomenon? Pharmacol Ther. 1992;53:375–408.
11 Key LL Jr, Ries WL, Taylor RG, Hays BD, Pitzer BL. Oxygen derived free radicals in osteoclasts: the specificity and location of the nitroblue tetrazolium reaction. Bone. 1990;11:115–119.
12 Garrett IR, Boyce BF, Oreffo RO, Bonewald L, Poser J, Mundy GR. Oxygen-derived free radicals stimulate osteoclastic bone resorption in rodent bone in vitro and in vivo. J Clin Invest. 1990;8:632–639.

13 Lee NK, Choi YG, Baik JY, Han SY, Jeong DW, Bae YS, et al. A crucial role for reactive oxygen species in RANKL-induced osteoclast differentiation. Blood. 2005;106:852–859.
14 Srinivasan S, Koenigstein A, Joseph J, Sun L, Kalyanaraman B, Zaidi M, et al. Role of mitochondrial reactive oxygen species in osteoclast differentiation. Ann N Y Acad. Sci. 2010;1192:245–252.
15 Ha H, Kwak HB, Lee SW, Jin HM, Kim HM, Kim HH, et al. Reactive oxygen species mediate RANK signaling in osteoclasts. Exp Cell Res. 2004;301:119–127.
16 Kajita M, Hikosaka K, Iitsuka M, Kanayama A, Toshima N, Miyamoto Y. Platinum nanoparticle is a useful scavenger of superoxide anion and hydrogen peroxide. Free Radic Res. 2007; 41:615–626.
17 Onizawa S, Aoshiba K, Kajita M, Miyamoto Y, Magai A. Platinum nanoparticle antioxidants inhibit pulmonary inflammation in mice exposed to cigarette smoke. Plum Pharmacol Ther. 2008;22:340–349.
18 Kim J, Takahashi M, Shimizu T, Shirasawa T, Kajita M, Kanayama A, et al. Effects of a potent antioxidant, platinum nanoparticle, on the lifespan of Caenorhabditis elegans. Mech Ageing Dev. 2008;129:322–331.
19 Kim J, Shirasawa T, Miyamoto Y. The effect of TAT conjugated platinum nanoparticles on lifespan in a nematode Caenorhabditis elegans model. Biomaterials. 2010;31:5849–5854.
20 Setsukinai K, Urano Y, Kakinuma K, Majima HJ, Nagano T. Development of novel fluorescence probes that can reliably detect reactive oxygen species and distinguish specific species. J Biol Chem. 2003;278:3170–3175.
21 Hikosaka K, Kim J, Kajita M, Kanayama A, Miyamoto Y. Platinum nanoparticles have an activity similar to mitochondrial NADH: ubiquinone oxidoreductase. Colloids Surf. 2008;66: 195–200.
22 Hu JP, Nishishita K, Sakai E, Yoshida H, Kato Y, Tsukuba T, et al. Berberine inhibits RANKL-induced osteoclast formation and survival through suppressing the NF-kappaB and Akt pathways. Eur J Pharmacol. 2008;580:70–79.
23 Suzuki N, Yoshimura Y, Deyama Y, Suzuki K, Kitagawa Y. Mechanical stress directly suppresses osteoclast differentiation in RAW264.7 cells. Int J Mol Med. 2008;21:291–296.
24 Bedard K, Krause KH. The NOX family of ROS-generating NADPH oxidases: physiology and pathophysiology. Physio Rev. 2007;87:245–313.
25 Lambeth JD, Kawahara T, Diebold B. Regulation of Nox and Duox enzymatic activity and expression. Free Radic Biol Med. 2007;43:319–331.
26 Katsuyama M. NOX/NADPH oxidase, the superoxide-generating enzyme: Its transcriptional regulation and physiological roles. J Pharmacol Sci. 2010;114:134–146.
27 Beckman KB, Ames BN. The free radical theory of aging matures. Physiol Rev. 1998;78:547–581.
28 Bokov A, Chaudhuri A, Richardson A. The role of oxidative damage and stress in aging. Mech Ageing Dev. 2004;125: 811–826.
29 Finkel T, Holbrook NJ. Oxidants, oxidative stress and the biology of ageing. Nature. 2000;408:239–247.
30 Zhao Q, Wang X, Liu Y, He A, Jia R. NFATc1: functions in osteoclasts. Int J Biochem Cell Biol. 2010;42:576–579.
31 Kim K, Lee SH, Kim JH, Choi Y, Kim N. NFATc1 induces osteoclast fusion via upregulation of Atp6v0d2 and the dendritic cell-specific transmembrane protein (DC-STAMP). Mol Endocrinol. 2008;22:176–185.
32 Yagi M, Miyamoto T, Sawatani Y, Iwamoto K, Hosogane N, Fujita N, et al. DC-STAMP is essential for cell-cell fusion in osteoclasts and foreign body giant cells. J Exp Med. 2005; 202:345–351.
33 Kitami S, Tanaka H, Kawato T, Tanabe N, Katono-Tani T, Zhang F, et al. IL-17A suppresses the expression of bone resorption-related proteinases and osteoclast differentiation via IL-17RA or IL-17RC receptors in RAW264.7 cells. Biochimie. 2010;92: 398–404.
34 Shibata K, Yoshimura Y, Kikuiri T, Hasegawa T, Taniguchi Y, Deyama Y, et al. Effect of the release from mechanical stress on osteoclastogenesis in RAW264.7 cells. Int J Mol Med. 2011; 28:73–79.
35 Steinbeck MJ, Appel WH, Verhoeven AJ, Karnovsky MJ. NADPH-oxidase production of superoxide by osteoclasts actively resorbing bone. J Cell Biol. 1994;126:765–772.
36 Yang S, Ries WL, Key LL. NADPH oxidase in the formation of superoxide in osteoclasts. Calcif Tissue Int. 1998;63:346–350.
37 Sasaki H, Yamamoto H, Tominaga K, Masuda K, Kawai T, Teshima-Kondo S, et al. Receptor activator of nuclear factor-κB ligand-induced mouse osteoclast differentiation is associated with switching between NADPH oxidase homologues. Free Radic Biol Med. 2009;47:189–199.
38 Yang S, Madyastha P, Bingel S, Ries W, Key L. A new superoxide-generating oxidase in murine osteoclasts. J Biol Chem. 2001;276:5452–5458.
39 Yang S, Zhang Y, Ries W, Key L. Expression of Nox4 in osteoclasts. J Cell Biochem. 2004;92:238–248.